

Few-body calculations of η -nuclear quasibound states

N. Barnea, E. Friedman, A. Gal*

Racah Institute of Physics, The Hebrew University, 91904 Jerusalem, Israel

Abstract

We report on precise hyperspherical-basis calculations of ηNN and ηNNN quasibound states, using energy dependent ηN interaction potentials derived from coupled-channel models of the S_{11} $N^*(1535)$ nucleon resonance. The ηN attraction generated in these models is too weak to generate a two-body bound state. No ηNN bound-state solution was found in our calculations in models where $\text{Re } a_{\eta N} \lesssim 1$ fm, with $a_{\eta N}$ the ηN scattering length, covering thereby the majority of $N^*(1535)$ resonance models. A near-threshold ηNNN bound-state solution, with η separation energy of less than 1 MeV and width of about 15 MeV, was obtained in the 2005 Green-Wycech model where $\text{Re } a_{\eta N} \approx 1$ fm. The role of handling self consistently the subthreshold ηN interaction is carefully studied.

Keywords: few-body systems, mesic nuclei, forces in hadronic systems and effective interactions

1. Introduction

The ηN interaction has been studied extensively in photon- and hadron-induced production experiments on free and quasi-free nucleons, and on nuclei [1]. These experiments suggest that the near-threshold ηN interaction is attractive, but are unable to quantify this statement in any precise manner. Nevertheless, η production data on nuclei provide some useful hints on possible η quasibound states for very light species where, according to Krusche and Wilkin (KW) “the most straightforward (but not unique) interpretation of the data is that the ηd system is unbound, the $\eta^4\text{He}$ is bound, but that

*corresponding author: Avraham Gal, avragal@savion.huji.ac.il

the $\eta^3\text{He}$ case is ambiguous” [1]. Indeed, the prevailing theoretical consensus since the beginning of the 2000s, based on ηNN Faddeev calculations, is that ηd quasibound or resonance states are ruled out for acceptable ηN interaction strengths [2, 3]. Instead, the ηd system may admit virtual states [4, 5, 6]. Searching for reliable few-body calculations of the $A = 3, 4$ η -nuclear systems, we are aware of none for $\eta NNNN$ and of only one ηNNN Faddeev-Yakubovsky calculation [7], although not sufficiently realistic, that finds no $\eta^3\text{H}$ quasibound state. Rigorous few-body calculations substantiating the KW conjecture quoted above are therefore called for. The present work fills some of this gap, reporting precise calculations of ηNN and of ηNNN few-body systems using the hyperspherical basis methodology [8], similarly to the calculations reported in Ref. [9] for the $\bar{K} NN$ and $\bar{K} NNN$ systems. Particular attention is given in the present work to the subthreshold energy dependence of the ηN interaction in a way not explored before in η few-body calculations.

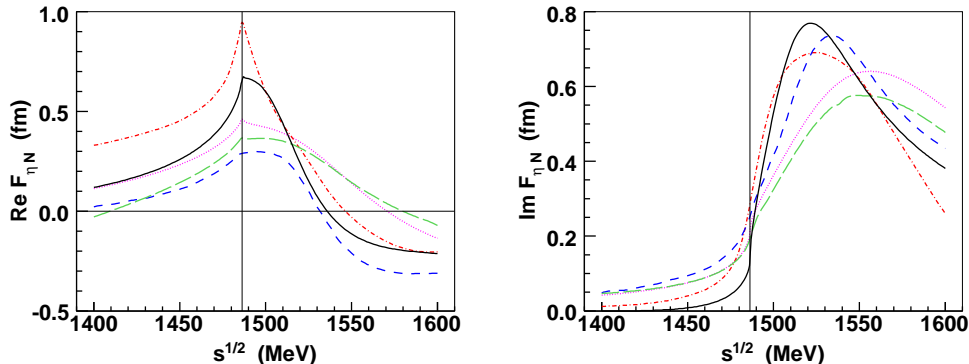


Figure 1: Real (left panel) and imaginary (right panel) parts of the ηN cm scattering amplitude $F_{\eta N}(\sqrt{s})$ as a function of the total cm energy \sqrt{s} in five meson-baryon coupled-channel interaction models, in decreasing order of $\text{Re } a_{\eta N}$. Dot-dashed curves: GW [11]; solid: CS [12]; dotted: KSW [13]; long-dashed: M2 [14]; short-dashed: IOV [15]. The thin vertical line denotes the ηN threshold. Figure adapted from [16].

Theoretically, the ηN interaction has been studied in coupled-channel models that seek to fit or, furthermore, generate dynamically the prominent $N^*(1535)$ resonance which peaks about 50 MeV above the ηN threshold. Such models result in a wide range of values for the real part of the ηN scattering length $a_{\eta N}$, from 0.2 fm [10] to almost 1.0 fm [11]. Most of these

analyses constrain the imaginary part $\text{Im } a_{\eta N}$ within a considerably narrower range of values, from 0.2 to 0.3 fm. This is demonstrated in Fig. 1 where the real and imaginary parts of the ηN center-of-mass (cm) scattering amplitude $F_{\eta N}(\sqrt{s})$ are plotted as a function of the cm energy \sqrt{s} for several coupled channel models. The ηN threshold, where $F_{\eta N}(\sqrt{s_{\text{th}}}) = a_{\eta N}$, is denoted by a thin vertical line. We note that both real and imaginary parts of $F_{\eta N}(\sqrt{s})$ below threshold decrease monotonically in all of these models upon going deeper into the subthreshold region, displaying however substantial model dependence. This will become important for the η few-body calculations reported here.

Beginning with the pioneering work by Haider and Liu [17], and using input values of $a_{\eta N}$ within these specified ranges, several η -nucleus optical-model bound-state calculations concluded that η mesons are likely to bind in sufficiently heavy nuclei, certainly in ^{12}C and beyond [18, 19, 20, 21, 22]. In the few-body calculations reported here we find no ηd quasibound states for values of $\text{Re } a_{\eta N}$ as large as about 1 fm. We do find, however, a very weakly bound and broad $\eta^3\text{H}-\eta^3\text{He}$ isodoublet pair for $\text{Re } a_{\eta N} \approx 1$ fm by solving the ηNNN four-body problem.

The paper is organized as follows. In section 2 we construct local energy-dependent single-channel potentials $v_{\eta N}$ that reproduce two of the s -wave scattering amplitudes $F_{\eta N}(\sqrt{s})$ shown in Fig. 1, GW [11] and CS [12]. In section 3 we sketch the hyperspherical-basis formulation and solution of the ηNN and ηNNN Schroedinger equations below threshold using these derived ηN potentials and realistic energy-independent NN potentials. Because of the substantial energy dependence of $v_{\eta N}$ in the subthreshold region, a self consistency requirement [9] is applied so that the input energy argument of the two-body potential $v_{\eta N}$ for convergent few-body solutions is consistently related to some energy expectation values in the resulting quasibound state. Results are presented and discussed in section 4, followed by a brief summary and outlook section 5.

2. Construction of ηN effective potentials

We seek to construct energy-dependent local ηN potentials $v_{\eta N}$ that reproduce the ηN scattering amplitude $F_{\eta N}(\sqrt{s})$ below threshold in given models, e.g. from among those shown in Fig. 1. For convenience, the energy argument E introduced in this section is defined with respect to the ηN threshold,

$E \equiv \sqrt{s} - \sqrt{s_{\text{th}}}$, and should not be confused with the binding energy of the ηNN and ηNNN few-body states studied in subsequent sections.

We define $v_{\eta N}$ in the form

$$v_{\eta N}(E; r) = -\frac{4\pi}{2\mu_{\eta N}} b(E) \rho_{\Lambda}(r), \quad (\hbar = c = 1) \quad (1)$$

with $\mu_{\eta N}$ the reduced ηN mass and where ρ_{Λ} is a Gaussian normalized to 1:

$$\rho_{\Lambda}(r) = \left(\frac{\Lambda}{2\sqrt{\pi}} \right)^3 \exp\left(-\frac{\Lambda^2 r^2}{4} \right). \quad (2)$$

Λ is a scale parameter, inversely proportional to the range of $v_{\eta N}$. Its physically admissible values are discussed in subsection 2.2 below. Two representative values are used here, $\Lambda=2$ and 4 fm^{-1} . For a given value of Λ , one needs to determine the energy-dependent strength parameter $b(E)$ of $v_{\eta N}$, as described in the following subsection 2.1.

2.1. Solution

Given a specific value of the scale parameter Λ , the two-body s -wave Schroedinger equation

$$-\frac{1}{2\mu_{\eta N}} u''(r) + v_{\eta N}(E; r)u(r) = Eu(r) \quad (3)$$

is solved for energies above ($E > 0$) and below ($E < 0$) threshold. The radial wavefunction $u(r)$ satisfies the boundary conditions

$$u(r=0) = 0, \quad u(r \rightarrow \infty) \propto r(\cos \delta_0 j_0(kr) - \sin \delta_0 n_0(kr)), \quad (4)$$

where $k = \sqrt{2\mu_{\eta N} E}$, j_0 and n_0 are spherical Bessel and Neumann functions, respectively, and $\delta_0(E)$ is the complex s -wave phase shift derived by imposing these boundary conditions on the wave-equation solution. Above threshold, the wave number k is real and taken positive. Below threshold, $k = i\kappa$ with $\kappa > 0$. The scattering amplitude F is then given by

$$F_{\eta N}(E) = \frac{1}{k(\cot \delta_0 - i)}. \quad (5)$$

This procedure was used in Ref. [23] for constructing effective $\bar{K}N$ potentials below threshold. In the present case, the subthreshold values of the complex

strength parameter $b(E)$ in Eq. (1) were fitted to the complex phase shifts $\delta(E)$ derived from subthreshold scattering amplitudes $F_{\eta N}(E)$ in several of the coupled-channel models of Fig. 1. This is shown for the GW [11] and CS [12] models in Fig. 2, using two values of the scale parameter $\Lambda=2$ and 4 fm^{-1} for GW and just one value $\Lambda = 4 \text{ fm}^{-1}$ for CS. The curves $b(E)$ are seen to decrease monotonically in going deeper below threshold, except for small kinks near threshold that reflect the threshold cusp of $\text{Re } F_{\eta N}(E = 0)$ in Fig. 1. Comparing models GW and CS for the *same* scale parameter $\Lambda = 4 \text{ fm}^{-1}$, one observes larger values of $b(E)$ in model GW than in CS, for both real and imaginary parts below threshold, in line with the larger GW subthreshold amplitudes compared with the corresponding CS amplitudes. We note furthermore that $\text{Im } b(E) \ll \text{Re } b(E)$ in both models by almost an order of magnitude, see Fig. 2, which justifies treating $\text{Im } v_{\eta N}$ perturbatively in the applications presented below.

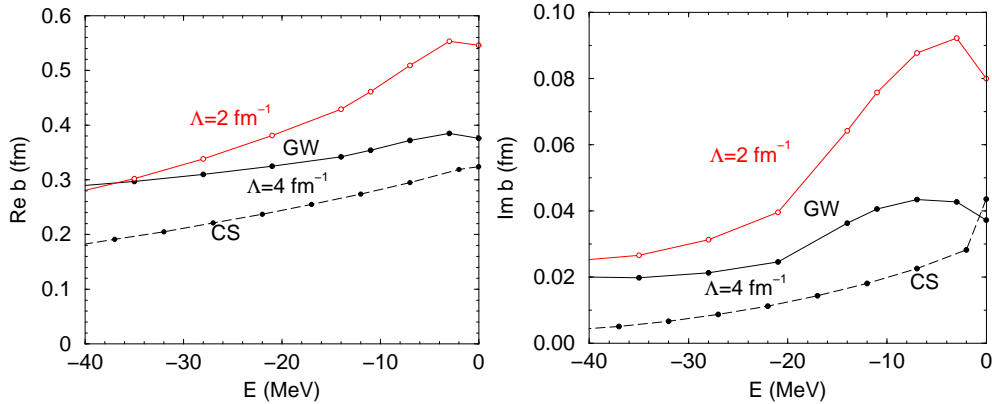


Figure 2: Real (left panel) and imaginary (right panel) parts of the strength parameter $b(E)$ of the ηN effective potential (1), for subthreshold energies $E < 0$, obtained from the scattering amplitudes $F_{\eta N}^{\text{GW}}$ [11] and $F_{\eta N}^{\text{CS}}$ [12] shown in Fig. 1. Two choices of the scale parameter Λ are made for GW, both resulting in the same $F_{\eta N}^{\text{GW}}(E)$, and just one for CS.

To demonstrate the extent to which the energy dependence of $b(E)$ is essential, we compare in Fig. 3 the GW subthreshold amplitude from Fig. 1, which is also generated here using the $b(E)$ potential strength of Fig. 2 for $\Lambda = 4 \text{ fm}^{-1}$, to the amplitude marked gw which was calculated using a fixed threshold value $b(E = 0)$. This latter amplitude is seen to decrease too slowly beginning about $E \approx -7 \text{ MeV}$. Obviously, an *energy-independent* single-

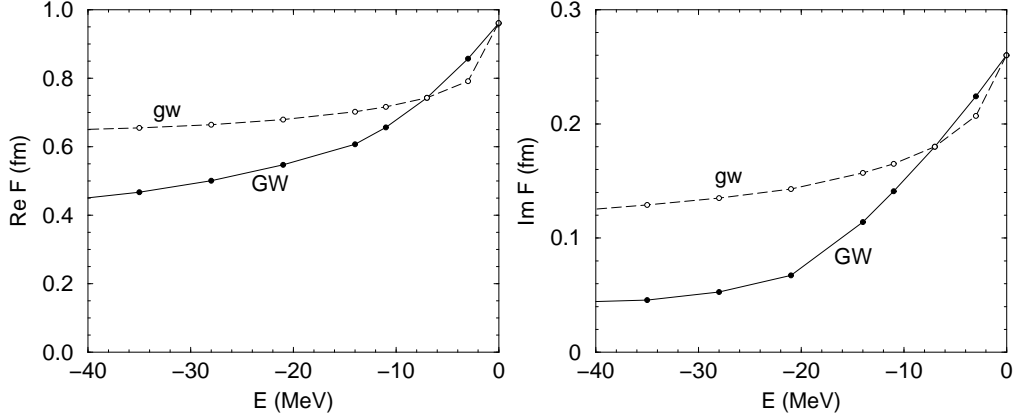


Figure 3: Real (left panel) and imaginary (right panel) parts of the subthreshold amplitude $F_{\eta N}^{\text{GW}}(E)$ (solid curves marked GW) from Fig. 1, also generated from an energy dependent potential $v_{\eta N}^{\text{GW}}(E)$ with $\Lambda = 4 \text{ fm}^{-1}$, Eqs. (1,2), compared to the amplitude (dashed curves marked gw) generated from $v_{\eta N}^{\text{GW}}(E = 0)$.

channel potential $v_{\eta N}$ fails to reproduce the subthreshold energy dependence of the GW coupled-channel scattering amplitude $F_{\eta N}^{\text{GW}}(E)$.

2.2. Choice of scale

It is appropriate at this point to address the model dependence introduced in η -nuclear few-body calculations by the choice of the scale parameter Λ made in constructing $v_{\eta N}$, Eqs. (1) and (2). Λ is often identified with the momentum cutoff used to renormalize divergent loop integrals in on-shell EFT $N^*(1535)$ models [14, 15]. In separable-interaction coupled channel models, however, the momentum cutoff is replaced by fitted Yamaguchi form factors $(q^2 + \Lambda^2)^{-1}$ with a momentum-space range parameter Λ , the Fourier transform of which is a Yukawa potential $\exp(-\Lambda r)/r$ with r.m.s radius identical to that of the Gaussian potential shape (2). Values of Λ from three such $N^*(1535)$ models, including the two used in the present work [11, 12], are listed in Table 1.

Inspection of Table 1 reveals a broad range of values that Λ may assume, starting with $\Lambda \approx 3 \text{ fm}^{-1}$. The relatively high value in the third column is rather exceptional for meson-baryon separable models. Given this broad spectrum of values spanned for Λ , we chose two values $\Lambda = 2$ and $\Lambda = 4 \text{ fm}^{-1}$ to study the model dependence of our η -nuclear few-body calculations. The

Table 1: The ηN momentum scale parameter Λ from several $N^*(1535)$ separable models.

Ref.	[10, 13]	[11]	[12]
Λ (fm $^{-1}$)	3.9	3.2	6.6

higher value, $\Lambda = 4$ fm $^{-1}$, corresponds to a Gaussian $\exp(-r^2/R^2)$ spatial range $R = 2/\Lambda = 0.5$ fm, a value which is very close to $R = 0.47$ fm taken from the systematic EFT approach in Ref. [23] and used in our \bar{K} -nuclear few-body calculations [9]. As argued there, choosing smaller values for R , namely larger values than 4 fm $^{-1}$ for Λ , would be inconsistent with staying within a purely hadronic basis.¹

In the Introduction section we loosely identified the strength of the ηN interaction with the size of the real part of its threshold scattering amplitude, $\text{Re } a_{\eta N} \lesssim 1$ fm. However, in terms of the interaction potentials $v_{\eta N}$ that enter our few-body calculations, a given value of $\text{Re } a_{\eta N}$ does not rule out a broad spectrum of spatial ranges, or equivalently momentum scale parameters Λ , as demonstrated in Fig. 2. A model dependence is thereby introduced into our few-body calculations, summarized by stating that the larger the ηN scale parameter Λ is, the larger is the η separation energy, provided it is quasibound. This lack of scale invariance hints towards the necessity of including three-body forces, as is expected from an EFT point of view [25]. Such three-body forces amount to adding a new free parameter determined by tuning it to some η few-body experimental data.

¹The effective energy-dependent $\bar{K}N$ potential $v_{\bar{K}N}$ constructed by Hyodo and Weise [23] reproduces the $\bar{K}N - \pi\Sigma$ coupled-channel scattering amplitude which is the one essential for generating dynamically the $\Lambda^*(1405)$ resonance. In that case, the choice of Λ must ensure that the \bar{K}^*N channel that couples strongly to $\bar{K}N$ via normal pion exchange is kept outside of the model space in which $v_{\bar{K}N}$ is valid. This argument leads to a choice of $\Lambda = p_{\min}(\bar{K}N \rightarrow \bar{K}^*N) = 552$ MeV/c or 2.8 fm $^{-1}$, corresponding to a Gaussian spatial range of $R = 0.71$ fm. In a somewhat similar reasoning Garzon and Oset [24] recently argued for extending the EFT description of the $N^*(1535)$ resonance to include the ρN channel which couples strongly to the already included πN channel, although not to ηN . Identifying Λ with the minimum momentum needed to excite the πN system to ρN , we obtain $\Lambda = p_{\min}(\pi N \rightarrow \rho N) = 586$ MeV/c or 3.0 fm $^{-1}$.

3. η -nuclear hyperspherical-basis formulation and solution

The hyperspherical-basis formulation of meson-nuclear few-body calculations was initiated in Ref. [9] for \bar{K} mesons. Here we sketch briefly the necessary transformation from \bar{K} mesons to η mesons. The N -body wavefunction ($N = 3, 4$) in our case consists of a sum over products of isospin, spin and spatial components, antisymmetrized with respect to nucleons. In the spatial sector translationally invariant basis functions are constructed in terms of one hyper-radial coordinate ρ and a set of $3N - 4$ angular coordinates $[\Omega_N]$, substituting for $N - 1$ Jacobi vectors. The spatial basis functions are of the form

$$\Phi_{n,[K]}(\rho, \Omega_N) = R_n^N(\rho) \mathcal{Y}_{[K]}^N(\Omega_N), \quad (6)$$

where $R_n^N(\rho)$ are hyper-radial basis functions expressible in terms of Laguerre polynomials and $\mathcal{Y}_{[K]}^N(\Omega_N)$ are hyperspherical-harmonics (HH) functions in the angular coordinates Ω_N expressible in terms of spherical harmonics and Jacobi polynomials. Here, the symbol $[K]$ stands for a set of angular-momentum quantum numbers, including those of \hat{L}^2 , \hat{L}_z and \hat{K}^2 , where $\hat{\mathbf{K}}$ is the total grand angular momentum which reduces to the total orbital angular momentum for $N = 2$. The HH functions $\mathcal{Y}_{[K]}^N$ are eigenfunctions of \hat{K}^2 with eigenvalues $K(K + 3N - 5)$, and $\rho^K \mathcal{Y}_{[K]}^N$ are harmonic polynomials of degree K [8].

For the NN interaction we used two forms, the (Minnesota) MN central potential [26] and the Argonne AV4' potential [27] derived from the full AV18 potential by suppressing the spin-orbit and tensor interactions and readjusting the central spin and isospin dependent interactions. In s -shell nuclei the AV4' potential provides an excellent approximation to AV18 which pseudoscalar mesons, such as the η meson, are unlikely to spoil, recalling that their nuclear interactions cannot induce $S \leftrightarrow D$ mixing beyond that already accounted for by the NN interaction.² AV4' and MN differ mostly in their short-range repulsion which is much stronger in AV4' than in MN.

For the ηN interaction we used the energy-dependent local potential Re $v_{\eta N}$ introduced in Sect. 2. In order to distinguish the energy E of the

²This was demonstrated in \bar{K} nuclear cluster calculations [9], see the discussion of Table 1 therein, where the $\bar{K}(NN)_{I=0}$ 4.7 MeV binding energy contribution to the full 15.7 MeV binding energy of $(\bar{K}NN)_{I=1/2}$ calculated using AV4' is short by only 0.2 MeV from that in a comparable calculation [28] using AV18.

few-body system from the energy argument of $v_{\eta N}$, the latter is replaced by $\delta\sqrt{s} \equiv \sqrt{s} - \sqrt{s_{\text{th}}}$ from now on. Following Eq. (5) in [9], the subthreshold energy argument $\delta\sqrt{s}$ of $v_{\eta N}$, is chosen to agree self-consistently with

$$\langle\delta\sqrt{s}\rangle = -\frac{B}{A} - \xi_N \frac{A-1}{A} \langle T_{N:N} \rangle - \frac{A-1}{A} B_\eta - \xi_\eta \left(\frac{A-1}{A} \right)^2 \langle T_\eta \rangle, \quad (7)$$

where $\xi_{N(\eta)} \equiv m_{N(\eta)}/(m_N + m_\eta)$, T_η is the η kinetic energy operator in the total cm frame, $T_{N:N}$ is the pairwise NN kinetic energy operator in the NN pair cm frame, B is the total binding energy of the η -nuclear few-body system and B_η is the η “binding energy”, $B_\eta \equiv -E_\eta = -\langle\Psi|(H - H_N)|\Psi\rangle$, where H_N is the Hamiltonian of the purely nuclear part in its own cm frame and the total Hamiltonian H is evaluated in the overall cm frame. In the limit $A \gg 1$, Eq. (7) agrees with the nuclear-matter expression given in Refs. [21, 22] for use in calculating η -nuclear quasibound states. It provides a self-consistency cycle in η -nuclear few-body calculations by requiring that the expectation value $\langle\delta\sqrt{s}\rangle$ derived from the solution of the Schroedinger equation agrees with the input value $\delta\sqrt{s}$ used in $v_{\eta N}$. Since each one of the four terms on the r.h.s. of (7) is negative, the self consistent energy shift $\delta\sqrt{s_{\text{s.c.}}}$ is necessarily negative, with size exceeding a minimum nonzero value obtained from the first two terms in the limit of vanishing η binding.

The potential and kinetic energy matrix elements for a given η -nuclear state with global quantum numbers I, L, S, J^π were evaluated in the HH basis. The NN and ηN interactions specified above conserve $I = I_N$, $S = S_N$ and L . Since no $L \neq 0$ η -nuclear states are likely to come out particle stable, our calculations are limited to $L = 0$. The deuteron in this approximation is a purely 3S_1 state. Suppressing $\text{Im } v_{\eta N}$, the g.s. energy $E_{\text{g.s.}}$ was calculated in a model space spanned by HH basis functions with eigenvalues $K \leq K_{\text{max}}$. Self-consistent calculations were done for \sqrt{s} ranging from the ηN threshold down to 30 MeV below. Self consistency in $\delta\sqrt{s}$ was reached after a few cycles. Good convergence was achieved for values of $K_{\text{max}} \approx 20 - 40$. Asymptotic values of $E_{\text{g.s.}}$ were found by fitting the constants C and α of the parametrization

$$E(K_{\text{max}}) = E_{\text{g.s.}} + C \exp(-\alpha K_{\text{max}}) \quad (8)$$

to values of $E(K_{\text{max}})$ calculated for sufficiently high values of K_{max} . The accuracy reached is better than 0.1 MeV in both the three-body and the four-body calculations reported here.

The conversion width Γ was then evaluated through the expression

$$\Gamma = -2 \langle \Psi_{\text{g.s.}} | \text{Im } V_{\eta N} | \Psi_{\text{g.s.}} \rangle, \quad (9)$$

where $V_{\eta N}$ sums over all pairwise ηN interactions. Since $|\text{Im } V_{\eta N}| \ll |\text{Re } V_{\eta N}|$, this is a reasonable approximation for the width.

4. Results and discussion

Results of ηNN and ηNNN bound-state hyperspherical-based calculations for the GW ηN interaction, with $\text{Re } a_{\eta N}$ almost 1 fm, are given in this section. The weaker CS ηN interaction is found too weak to generate bound-state solutions.

4.1. ηNN calculations

No $I = 0$, $J^\pi = 1^-$ ηd bound state solution was found for the ηNN three-body system using the MN NN potential [26] and the GW [11] ηN effective potential with a fixed strength $b(\delta\sqrt{s} = 0)$, see Fig. 2, for either choice $\Lambda = 2$ or 4 fm^{-1} of the scale parameter under study. It was found that $b(\delta\sqrt{s} = 0)$ in the GW model needs to be multiplied by 1.1 for $\Lambda = 4 \text{ fm}^{-1}$ and by 1.3 for $\Lambda = 2 \text{ fm}^{-1}$ in order to generate a 1^- ηNN weakly bound state, with overall binding energy of -2.219 and -2.264 MeV, respectively, within three-body calculations that use a fixed ηN interaction strength $b(\delta\sqrt{s} = 0)$. Recall that the MN deuteron binding energy is $E_d = -2.202$ MeV. There is no ηd bound state also in the ηN CS [12] model, judging by the CS/GW relative strengths of $b(\delta\sqrt{s})$.

Given that the ηN interaction is too weak to bind the $I = 0$, $J^\pi = 1^-$ ηNN state in which the 3S_1 NN (deuteron) core configuration is bound, the unbound 1S_0 NN core configuration in the $I = 1$, $J^\pi = 0^-$ ηNN state certainly cannot support a three-body bound state. This holds so long as the 1^- state is unbound and also for a certain range of larger ηN potential strengths that make the 1^- bound. This situation is reminiscent of the ΛNN system which is known to have *one* $I = 0$ bound state in which the Λ hyperon is bound to a deuteron core, but no $I = 1$ ΛNN bound state, see e.g. Ref. [29].

Our negative results rule out any ηd bound state, practically in all dynamical models of the $N^*(1535)$ resonance where the ηN interaction is coupled in, and are consistent with similar conclusions reached in Refs. [2, 3, 4, 5, 6].

This holds also upon replacing the MN NN interaction [26] by the AV4' NN interaction [27] in our ηNN calculations. In fact, somewhat larger ηN interaction multiplicative factors are then required to reach the onset of ηNN binding compared to those specified above. Applying the self-consistency requirement discussed in Sect. 3 to the ηNN calculation, and recalling the decreased strength $b(\delta\sqrt{s})$ in the ηN subthreshold region, see Fig. 2, would only aggravate the failure to generate a three-body ηNN bound state.

4.2. ηNNN calculations

Four-body ηNNN calculations were made using the MN [26] and the AV4' [27] NN potentials, and the GW [11] and CS [12] energy-dependent ηN potentials from Sect. 2. Based on $\eta^3\text{H}$ and $\eta^3\text{He}$, and with the leading $3N$ configuration given by $I_N = S_N = \frac{1}{2}$ and $L_N^\pi = 0^+$, the quantum numbers of the calculated ηNNN state are $I = S = \frac{1}{2}$, $L = 0$ and $J^\pi = \frac{1}{2}^-$. The $3N$ binding energy (disregarding the Coulomb interaction in the case of ${}^3\text{He}$) within our hyperspherical-basis calculation is -8.38 MeV for MN and -8.99 MeV for AV4'. Starting with the ηN GW model, with $\text{Re } a_{\eta N} = 0.96$ fm, and using the corresponding $v_{\eta N}$ from Sect. 2 with *energy independent* threshold strength $b(\delta\sqrt{s} = 0)$ for $\Lambda = 4 \text{ fm}^{-1}$, a four-body ηNNN bound state was found with η separation energy $E_{\text{g.s.}}^{\text{no s.c.}}$ between 2 to 3 MeV, as listed in Table 2. We then applied a self consistency procedure by doing calculations with several given values of strength $b(\delta\sqrt{s})$, requiring that the expectation value $\langle\delta\sqrt{s}\rangle$ evaluated by Eq. (7) from the obtained solution agrees with the input value of the subthreshold energy $\delta\sqrt{s}$ argument of the strength $b(\delta\sqrt{s})$ used in the calculation. This resulted in considerably reduced values of less than 1 MeV for the η separation energy $E_{\eta \text{ sep.}}^{\text{s.c.}}$ which are listed in Table 2, together with the corresponding ηNNN binding energies $E_{\text{g.s.}}^{\text{s.c.}}$. Also listed in the table are the self consistent values $\delta\sqrt{s_{\text{s.c.}}}$ and the self-consistency reduction factors $x_{\text{s.c.}} \equiv b(\delta\sqrt{s_{\text{s.c.}}})/b(\delta\sqrt{s} = 0)$. No ηNNN bound-state solutions were found using $v_{\eta N}^{\text{GW}}$ self consistently for $\Lambda = 2 \text{ fm}^{-1}$.

Table 2: Results of ηNNN quasibound-state self-consistent calculations using the ηN model GW [11]. Energies and widths are given in MeV.

NN int.	$E(\text{NNN})$	$E_{\text{g.s.}}^{\text{no s.c.}}$	$\delta\sqrt{s_{\text{s.c.}}}$	$x_{\text{s.c.}}$	$E_{\text{g.s.}}^{\text{s.c.}}$	$E_{\eta \text{ sep.}}^{\text{s.c.}}$	$\Gamma_{\text{g.s.}}^{\text{s.c.}}$
MN	-8.38	-11.26	-13.52	0.914	-9.33	0.95	13.52
AV4'	-8.99	-11.33	-15.83	0.895	-9.03	0.04	15.75

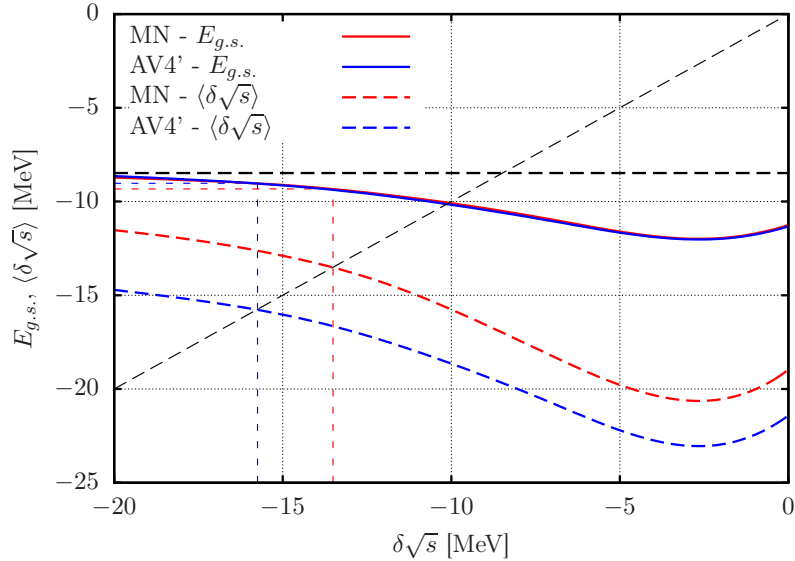


Figure 4: The ηNNN g.s. energy $E_{g.s.}$ (solid curves) and the expectation value $\langle \delta\sqrt{s} \rangle$ (dashed curves) from Eq. (7), calculated using the NN potentials MN (red) and AV4' (blue), are shown as a function of the energy argument $\delta\sqrt{s}$ used for the input $v_{\eta N}^{\text{GW}}$. The dashed horizontal line marks the NNN (${}^3\text{H}$) g.s. energy -8.48 MeV and the dashed diagonal line marks potentially self consistent solutions satisfying $\langle \delta\sqrt{s} \rangle = \delta\sqrt{s}$. The dashed vertical lines mark the intersection of the dashed diagonal line with the $\langle \delta\sqrt{s} \rangle$ dashed curves, thereby fixing the self-consistent values $\delta\sqrt{s_{s.c.}}$.

In order to demonstrate how the self consistency procedure works we plotted in Fig. 4 the ηNNN g.s. energy $E_{g.s.}$ and expectation value $\langle \delta\sqrt{s} \rangle$, calculated as a function of the subthreshold energy $\delta\sqrt{s}$ argument of the input ηN potential $v_{\eta N}$ in both NN potential models. The difference between the $E_{g.s.}$ curves, using MN or AV4', is a fraction of MeV for any given input value $\delta\sqrt{s}$ and is hardly noticeable in the figure. The difference between the corresponding $\langle \delta\sqrt{s} \rangle$ curves amounts to a few MeV at each value of $\delta\sqrt{s}$ and is clearly visible in the figure, leading to self-consistency values $\delta\sqrt{s_{s.c.}}$ which differ from each other by more than 2 MeV (marked by the dashed vertical lines). The corresponding self consistent values of $E_{g.s.}$ are much closer to each other (marked by the thin dashed horizontal lines). The self consistency procedure is applied in the figure by looking for the intersection of the dashed diagonal line, locus of $\langle \delta\sqrt{s} \rangle = \delta\sqrt{s}$, with each of the $\langle \delta\sqrt{s} \rangle$ dashed curves.

Applying a similar self-consistency procedure to the weaker CS ηN interaction, rather than to the GW ηN interaction used above, no ηNNN bound state solution was found. With AV4' for the NN interaction, this holds even upon using the threshold energy value in $v_{\eta N}^{\text{CS}}$. With the MN NN interaction and for the choice $\Lambda = 4 \text{ fm}^{-1}$, a bound-state solution is found for small values of the input energy $\delta\sqrt{s}$, disappearing at $-\delta\sqrt{s} \approx 2.8 \text{ MeV}$ which is way below the minimum value of $-\delta\sqrt{s}$ required in the limit of $E_{\eta \text{ sep.}} \rightarrow 0$. We conclude that the CS ηN interaction is too weak to provide self consistently ηNNN bound states.

Finally, the ηNNN width $\Gamma_{\text{g.s.}}^{\text{s.c.}} \sim 15 \text{ MeV}$ listed in the last column of Table 2 was calculated using $\text{Im } b(\delta\sqrt{s_{\text{s.c.}}})$ in forming the integrand $\text{Im } V_{\eta N}$ in Eq. (9). This width is about three times larger than the widths evaluated self consistently using optical model methods across the periodic table within the ηN GW model [21]. Some explanation of this difference is offered noting that the magnitude of the downward energy shifts $\delta\sqrt{s_{\text{s.c.}}}$ effective in those works is considerably larger by factors of two to three than the $\approx 15 \text{ MeV}$ found in the present ηNNN calculations, reflecting the denser nuclear environment encountered by the η meson as it becomes progressively more bound in the calculations of Ref. [21]. Recalling the steady decrease of the ηN absorptivity $\text{Im } F_{\eta N}$ in Fig. 1 upon moving deeper into subthreshold energies, a factor of two to three difference could be anticipated in favor of relatively small η widths in heavier nuclei.

5. Summary and outlook

Precise hyperspherical-based few-body calculations were reported in this work to explore computationally whether or not η mesons bind in light nuclei. To this end, complex energy-dependent local effective ηN potentials $v_{\eta N}$ were constructed, for subthreshold energies relevant to η mesic nuclei, from coupled channel ηN scattering amplitudes in several models connected dynamically to the $N^*(1535)$ resonance. The scale dependence arising from working with an effective $v_{\eta N}$ was studied by using two representative values for the momentum scale, $\Lambda = 2, 4 \text{ fm}^{-1}$. Noting that $\text{Im } v_{\eta N} \ll \text{Re } v_{\eta N}$, only the real part of $v_{\eta N}$ was used in the bound-state calculations, with a related error estimated as less than 0.2 MeV, added to an estimated 0.1 MeV calculational error. The width of the bound state, making it into a quasi-bound state, was deduced from the expectation value of $\text{Im } v_{\eta N}$ summed on all nucleons.

No ηNN quasibound states were found for any of the two scale parameters chosen in models where the real part of the ηN threshold interaction satisfies $\text{Re } a_{\eta N} \lesssim 1$ fm, in agreement with deductions made in several past few-body calculations of the ηd scattering length [2, 3, 4, 5, 6]. It is unlikely that the ηd system can reach binding upon increasing moderately the momentum scale parameter Λ .

For ηNNN , essentially the $\eta^3\text{H}$ and $\eta^3\text{He}$ isodoublet of η mesic nuclei, a relatively broad and weakly bound state was found with η separation energy of less than 1 MeV using the GW ηN interaction model [11] where $\text{Re } a_{\eta N}$ is almost 1 fm. This holds for the larger of the two values of momentum scale parameter, $\Lambda = 4 \text{ fm}^{-1}$, studied here, whereas no bound state was obtained upon using the smaller value of $\Lambda = 2 \text{ fm}^{-1}$. The energy dependence of $v_{\eta N}^{\text{GW}}$, treated here within a self consistent procedure [21, 22], played an important role by reducing the calculated binding energy by about 2 MeV from that calculated upon using the ηN threshold energy value in $v_{\eta N}^{\text{GW}}$. For such halo-like η -nuclear quasibound states, the neglect of $\text{Im } v_{\eta N}$ in the bound-state calculation requires attention. In the case of the GW ηN effective interaction, we estimate the repulsion added by reinstating $\text{Im } v_{\eta N}^{\text{GW}}$ to second order to be roughly $\lesssim 0.2$ MeV, eliminating thereby the very weakly bound ηNNN state calculated here using the AV4' NN potential, but not the weakly bound one calculated using the MN NN potential. It is worth noting that the only other few-body ηNNN study known to us [7] deduced from their calculated $\eta^3\text{H}$ scattering length that no quasibound state was likely. However, the strength of the ηN interaction tested in these calculations was limited to $\text{Re } a_{\eta N} = 0.75$ fm, short of our upper value of approximately 1 fm.

In conclusion, recalling the KW conjecture [1] quoted in the Introduction, it is fair to say that the present few-body calculations support the conjecture's first and last items, namely that “the ηd system is unbound” and “that the $\eta^3\text{He}$ case is ambiguous”. Accepting that the strength of the two-body ηN interaction indeed satisfies $\text{Re } a_{\eta N} \lesssim 1$ fm, which is much too weak to bind the ηN system, a persistent theoretical ambiguity connected with choosing a physically admissible range of values for the ηN scale parameter Λ is demonstrated by our few-body calculational results, particularly for the four-body ηNNN system. By choosing a considerably larger value of Λ than done here one could bind solidly this system. To remove this ambiguity, many-body repulsive interactions involving the η meson need to be derived and incorporated within few-body calculations.

In future work we hope to extend our ηNNN calculations also by applying

methods of complex scaling that should enable one to follow trajectories of S -matrix quasibound-state poles and look also for other types of poles such as virtual-state poles or resonance poles, all of which affect to some degree the threshold production features of η mesons in association with ${}^3\text{He}$. Furthermore we hope to initiate a precise and realistic calculation of the $\eta NNNN$ system in order to test the middle item in the KW conjecture, namely that “ $\eta^4\text{He}$ is bound”.

Acknowledgments

We thank Jiří Mareš for carefully reading this manuscript and making useful remarks. This work was supported in part (NB) by the Israel Science Foundation grant 954/09, and in part (EF, AG) by the EU initiative FP7, Hadron-Physics3, under the SPHERE and LEANNIS cooperation programs.

References

- [1] B. Krusche, C. Wilkin, *Prog. Part. Nucl. Phys.* 80 (2015) 43.
- [2] A. Deloff, *Phys. Rev. C* 61 (2000) 024004.
- [3] H. Garcilazo, M.T. Peña, *Phys. Rev. C* 61 (2000) 064010, 63 (2001) 021001(R).
- [4] A. Fix, H. Arenhövel, *Eur. Phys. J. A* 9 (2000) 119, *Nucl. Phys. A* 697 (2002) 277.
- [5] S. Wycech, A.M. Green, *Phys. Rev. C* 64 (2001) 045206
- [6] H. Garcilazo, *Phys. Rev. C* 67 (2003) 067001.
- [7] A. Fix, H. Arenhövel, *Phys. Rev. C* 66 (2002) 024002.
- [8] For a recent review of the hyperspherical basis methodology and other ones in few-body calculations, see W. Leidemann and G. Orlandini, *Prog. Part. Nucl. Phys.* 68 (2013) 158.
- [9] N. Barnea, A. Gal, E.Z. Liverts, *Phys. Lett. B* 712 (2012) 132.
- [10] N. Kaiser, T. Waas, W. Weise, *Nucl. Phys. A* 612 (1997) 297.

- [11] A.M. Green, S. Wycech, Phys. Rev. C 71 (2005) 014001, 72 (2005) 029902(E).
- [12] A. Cieplý, J. Smejkal, Nucl. Phys. A 919 (2013) 46.
- [13] N. Kaiser, P.B. Siegel, W. Weise, Phys. Lett. B 362 (1995) 23.
- [14] M. Mai, P.C. Bruns, U.-G. Meißner, Phys. Rev. D 86 (2012) 094033.
- [15] T. Inoue, E. Oset, M.J. Vicente Vacas, Phys. Rev. C 65 (2002) 035204.
- [16] A. Gal, E. Friedman, N. Barnea, A. Cieplý, J. Mareš, D. Gazda, Acta Phys. Pol. B 45 (2014) 673.
- [17] Q. Haider, L.C. Liu, Phys. Lett. B 172 (1986) 257; L.C. Liu, Q. Haider, Phys. Rev. C 34 (1986) 1845.
- [18] Q. Haider, L.C. Liu, Phys. Rev. C 66 (2002) 045208.
- [19] C. García-Recio, T. Inoue, J. Nieves, E. Oset, Phys. Lett. B 550 (2002) 47.
- [20] D. Jido, H. Nagahiro, S. Hirenzaki, Phys. Rev. C 66 (2002) 045202.
- [21] E. Friedman, A. Gal, J. Mareš, Phys. Lett. B 725 (2013) 334.
- [22] A. Cieplý, E. Friedman, A. Gal, J. Mareš, Nucl. Phys. A 925 (2014) 126.
- [23] T. Hyodo, W. Weise, Phys. Rev. C 77 (2008) 035204.
- [24] E.J. Garzon, E. Oset, Phys. Rev. C 91 (2015) 025201.
- [25] P.F. Bedaque, U. van Kolck, Annu. Rev. Nucl. Part. Sci. 52 (2002) 339.
- [26] D.R. Thompson, M. LeMere, Y.C. Tang, Nucl. Phys. A 286 (1977) 53.
- [27] R.B. Wiringa, S.C. Pieper, Phys. Rev. Lett. 89 (2002) 182501.
- [28] A. Doté, T. Hyodo, W. Weise, Nucl. Phys. A 804 (2008) 197, Phys. Rev. C 79 (2009) 014003.
- [29] A. Gal, H. Garcilazo, Phys. Lett. B 736 (2014) 93.